DOI: 10.4408/IJEGE.2011-03.B-028

THE EXPERIMENTAL STUDY ON THE GEOMETRIC SIMILARITY OF DEBRIS FLOW DEPOSITION

JINFENG LIU, GUOQIANG OU & YONG YOU(*)

Key Laboratory of Mountain Surface Process and Hazards, Chinese Academy of Sciences,Chengdu 610041, China; 2. Institute of Mountain Hazards and Environment, Chinese Academy of Sciences, Chengdu 610041, China. (*) Email: Liujf@imde.ac.cn

ABSTRACT

With the rapid development of the Chinese economy, many important building projects are planned on debris fans. Because of their location, these new constructions will be threatened by debris flows. Thus, it is important to study debris flow deposition in different conditions. Twenty debris fans under different experimental conditions are considered in order to examine the geometric similarity of debris flow deposition. The experimental results show that the cross-section, profile, and plane configuration of debris fans all have parabolic distributions. The quadratic term coefficients (a_1, a_2) of the debris fan cross-section and profile define the average deposition slope in the longitudinal and transverse directions. For the plane configuration, $-b_3/2a_3$ is the degree of deviation of the maximum downstream deposition width and c_3 is the ratio of the deposition width at the outlet to the maximum deposition width.

***KEY WORDS**: geometric similarity, debris flow, deposition, laboratory experiments*

INTRODUCTION

Debris flow is a sudden natural phenomenon, common in mountainous areas. Debris flows primarily cause erosion and deposition, particularly in the area of the debris fan. With the rapid development of the Chinese economy, many important transportation routes, water conservation and hydropower plants, towns, and factories have been built in, or are planned for, mountainous areas. Many of these projects have been or will be built on debris fans and thus will be threatened by debris flows. Therefore, the study of the geometric parameters of debris fan deposition is essential for organizing and implementing debris flow disaster prevention and mitigation plans.

To date, debris fan deposition prediction studies have mainly involved predicting debris flow volume (e.g., IKEYA, 1980; TANG, 1993; FRANZI, 2001; LIU, 2002), deposition length (e.g., PERLA *et alii*, 1980; CANNON, 1989; BENDA & CUNDY, 1990; ZIMMERMANN, 1991; WHIPPLE, 1992; PIERSON, 1995; BATHURST, 1997; IVERSON, 1998; VILLAR, 2000; FANNIN & WISE, 2001; LANCASTER, 2003; TOYOS, 2006), and alluvial area (BULL, 1964; CHRISTINE & ROBERT, 2003; BERTI and SIMONI, 2007). These studies have focused on making two dimensional predictions of debris flow deposition and lack a prediction of deposition depth. In order to make predictions in three dimensions, we must first consider the geometric parameters of debris flow deposition (XIE & CAI, 1998). XIE and CAI (1998) analyzed 72 debris deposition fans formed under different conditions and concluded that the non-dimensional longitudinal and cross-sectional profiles of debris flow fans can be described with Gaussian functions. In contrast, the non-dimensional plan form of debris flow fans can be described with a circular arc. However, the experimental fluid types employed were representative of stony and low viscosity debris flows. The geometric parameters of the viscous debris

flows that typically occur in southwestern China are still unknown. For this paper, a laboratory experiment is designed in order to analyze the geometric parameters of viscous debris flow deposition.

LABORATORY EXPERIMENT

EXPERIMENTAL APPARATUS AND MATERIAL

The experimental apparatus includes a hopper, flume, accumulation plate, and material recycling pool (Figure 1). The hopper measures 50 × 40 × 85 cm, with a capacity of 0.1 m³. The flume is a steel-truss structure with inside measurements of 20 × 30 cm, a valid flow length of 300 cm, and glass-reinforced sides to facilitate observation. The adjustable slope of the flume ranges from 0-20°. The accumulation plate is a rectangular steel-truss structure measuring 300 × 180 cm. A leveling board on the surface of the structure serves as an accumulation plane. The material recycling pool, a brick-molded rectangular pool, is positioned at the end of the accumulation plate. The pool measures 200 × 80 × 15 cm. the materials are cleaned after each experiment for reuse in the following experiment.

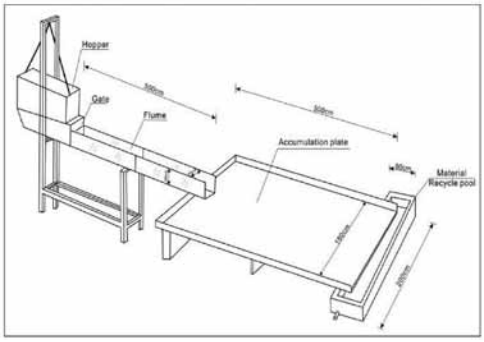

Fig. 1 - Experimental apparatus

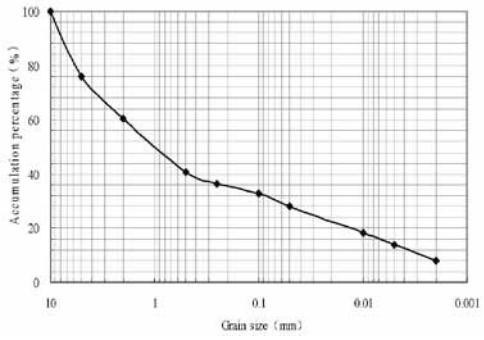

Fig. 2 - Particle gradation for the material used in the experiment

The experimental materials come from a sample of the original debris flow collected from the Jiangjia Gully, Dongchuan debris flow observation research station in Yunnan Province, China. The maximum grain size is 10 mm, the median grain size is 1.0 mm, and the average grain size is 3.25 mm (Figure 2).

SETTING

Twenty experiments in three groups, varying the scale and bulk density of the debris flow, and the slope of the accumulation area are conducted (Table 1).

PARAMETERS

The parameters of the debris flow are defined based on the results of experiment No.A_3 in Table 1 (Figures 3 and 5).

The X-axis is the cross-section direction, the Y axis is the profile direction, and the Z axis expresses deposition depth. Lc is the deposition length of the medial axis direction. Since the experimental deposition conditions are homogeneous and symmetrical,

No.	Scale V (cm^3)	Bulk density r_m (g/cm^3)	Slope of the accumulation area θ_d (°)
A_1	10,000	2.00	2.0
A_2	20,000	2.00	2.0
A_3	30,000	2.00	2.0
A_4	40,000	2.00	2.0
A_5	50,000	2.00	2.0
A_6	60,000	2.00	2.0
B_1	6,250	1.70	2.0
B_2	6,250	1.80	2.0
B_3	6,250	1.90	2.0
B_4	6,250	2.00	2.0
B_5	6,250	2.10	2.0
C_1	3,114	1.93	0.0
C_2	3,114	1.93	1.0
C_3	3,114	1.93	2.0
C_4	3,114	1.93	3.0
C_5	3,114	1.93	4.0
C_6	3,114	1.93	5.0
C_7	3,114	1.93	6.0
C_8	3,114	1.93	7.0
C_9	3,114	1.93	8.0

Tab. 1 - Experimental conditions

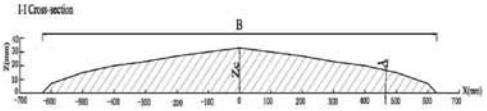

Fig. 3 - Cross-section parameters

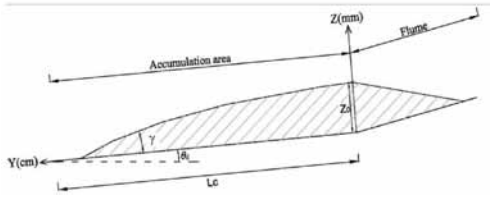

Fig. 4 - Profile parameters

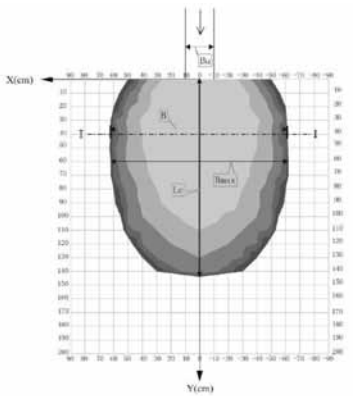

Fig. 5. Plane configuration parameters

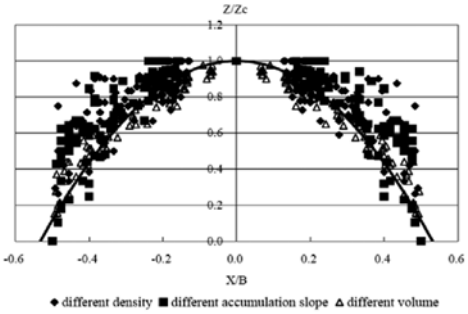

Fig. 6 - Relationship between dimensionless parameters Z/Zc and X/B

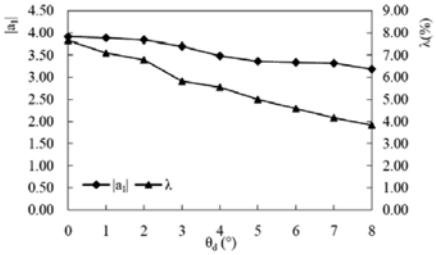

Fig. 7 - Relationship between $|a_1|$, λ and θ_d.

Lc is the maximum deposition length. B is the width of arbitrary cross section, Bmax is the maximum deposition width. Zc is the deposition depth of the center line of the cross section, Z_0 is the deposition depth of the midpoint of the flume outlet. In order to analyze the average deposition slope of the debris fan in the cross section and profile, λ is the transversal average deposition slope in the direction of the maximum deposition width (cross-section average deposition slope for short), γ is the average profile deposition slope in the direction of the maximum deposition length (average profile deposition slope for short), and θ_d is the slope of the accumulation area.

RESULTS AND DISCUSSION

GEOMETRIC SIMILARITY OF THE CROSS-SECTION

The relation between the dimensionless parameters Z/Zc and /B are shown in Figure 6.

Figure 6 shows that the cross-section of the debris fan under different conditions has a geometric similarity according to parabolic distribution. This can be expressed as follows:

$$Z / Zc = a_1 (X / B)^2 + b_1 (X / B) + c_1 \quad (1)$$

Since the debris fans in terms of a level and symmetrical deposition area are only considered in the experiments, Figure 6 indicates that the cross-section is a unary quadratic curve symmetrical around the Z/Zc axis. The vertex coordinate is (0,1).

Thus, $b_1 = 0$, $c_1 = 1$ in formula (1). The shape of the cross-section can be expressed as:

$$Z / Zc = a_1 (X / B)^2 + 1 \quad (2)$$

Next, we considered the relationship between quadratic coefficient a1 and debris fan deposition. Here, experimental group C in Table 1 as an example is used. The relationships between |a1|, the transversal average deposition slope (λ), and the slope of the accumulation area (θ_d) are shown in Figure 7.

Figure 7 shows that |a1| and λ have a negative, linear correlation with θ_d. As the accumulation slope increases, the maximum deposition width and depth decrease. Thus, the average crosssection deposition slope decreases as a result. Therefore, the quadratic coefficient, a_1, reflects the change in the transverse average deposition slope of the debris fan. The greater the absolute value, the greater the transverse average deposition slope.

GEOMETRIC SIMILARITY OF THE PROFILE

The relationship between the dimensionless parameters Zc/Z_0 and Y/Lc is shown in Figure 8.

Figure 8 shows that the debris fan profile also has a parabolic distribution. This can be expressed as:

$$Z_c / Z_0 = a_2 (Y / Lc)^2 + b_2 (Y / Lc) + c_2 \quad (3)$$

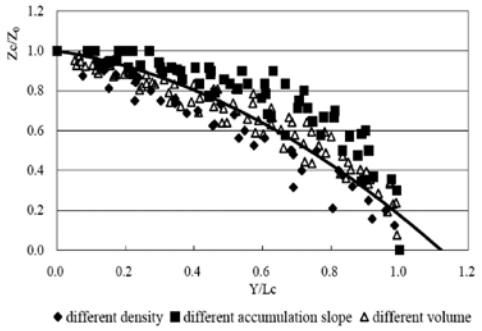

Fig. 8 - Relationship between dimensionless parameters Zc/Z_0 and Y/Lc

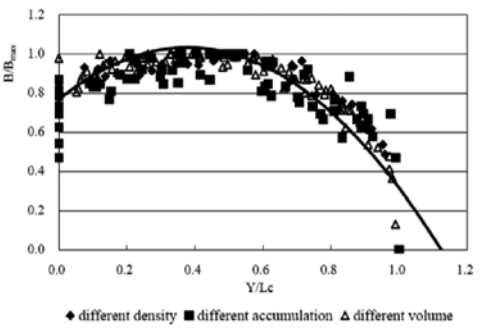

Fig. 10 - Relationship between dimensionless parameters B/B_{max} and Y/Lc

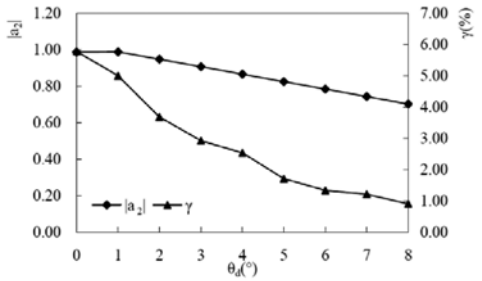

Fig. 9 - Relationship between $|a_2|$, γ and θ_d

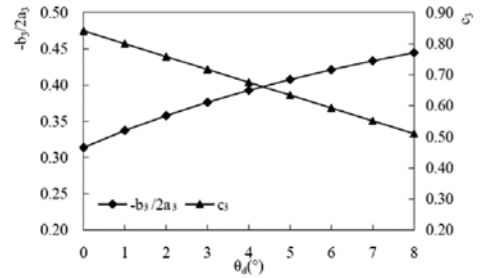

Fig. 11. Relationship between $-b_3/2a_3$, c_3 and θ_d

Since the debris fans in terms of a level and symmetrical deposition area are only considered, Figure 8 shows that the profile is a unary quadratic curve on the right side symmetrical around the Zc/Z_0 axis. The vertex coordinate is (0, 1). Thus, $b_2 = 0$, $c_2 = 1$ in formula (3). The shape of the profile can be expressed as:

$$Z_c / Z_0 = a_2 (Y / Lc)^2 + 1 \quad (4)$$

The relationship between $|a_2|$, the longitudinal average deposition slope (γ), and the slope of the accumulation area (θ_d) is shown in Figure 9.

Figure 9 shows that $|a_2|$ and γ have a negative, linear correlation with θ_d. As the accumulation slope increases, the maximum deposition length increases and the average deposition slope of the profile decreases. Therefore, the quadratic coefficient, a_2, reflects the change in the slope of the debris fan deposition. The greater the absolute value, the greater the longitudinal average deposition slope.

GEOMETRIC SIMILARITY OF THE PLANE CONFIGURATION

The relationship between the dimensionless parameters B/B_{max} and Y/Lc is shown in Figure 10.

Figure 10 shows that the plane configuration of the debris fan also has a parabolic distribution. This can be expressed as:

$$B / B_{max} = a_3 (Y / Lc)^2 + b_3 (Y / Lc) + c_3 \quad (5)$$

In the above formulas, $-b_3/2a_3$ is the axis symmetry and c_3 is the intercept of the curve. The relationship between $-b_3/2a_3$, c_3 and θ_d is shown in Figure 11.

Figure 11 indicates that as the accumulation slope increases, the position of the maximum width deviates further from the outlet. In summary, $-b_3/2a_3$ is the maximum degree of deviation of the downstream deposition width. The greater the value, the greater the deviation. c_3 is the ratio of the deposition width at the outlet of the gully to the maximum deposition width. The greater the value, the more similar is the deposition width at the outlet of the gully to the maximum width.

CONCLUSIONS

In this paper, twenty debris fans under different experimental conditions are examined in order to define the geometric similarity of viscous debris flow deposition. The results indicate that the crosssection, profile, and plane configuration of debris fans all have parabolic distributions. In addition, the physical meanings of the geometric similarity coefficients related to the geometry of debris fan cross-sections, profiles, and plane configurations are discussed.

The quadratic term coefficients (a_1 ,a_2) of the cross-section and profile define the average deposition slope of the debris fan in the longitudinal and transverse directions. The greater the value, the smaller the slope. For the plane configuration, $-b_3/2a_3$ is the degree of deviation of the maximum deposition width. The greater the value, the greater the deviation. c_3 is the ratio of the deposition width at the outlet to the maximum deposition width. The greater the value is, the more similar is the maximum deposition width and the deposition width at the outlet.

ACKNOWLEDGEMENTS

We are grateful for the technical support of Prof. Chjeng-Lun Shieh (Department of Hydraulic and Ocean Engineering, National Cheng Kung University, Taiwan, China) and Prof. Yuan-Fan Tsai (Social Studies Education, National Taipei University of Education, Taipei, Taiwan, China). This research was financially supported by the National Natural Science Foundation of China (40901008) and the Project group of the Knowledge Innovation Program (Kzcx2-Yw-Q03-5-2).

REFERENCES

A. Gomez-Villar & J.M.Garcia-Ruiz. (2000) - *Surface sediment characteristics and present dynamics in alluvial fans of the central Spanish Pyrenees*. Geomorphology, **34**: 127-144.

Bull W.B. (1964) - *Geomorphology of segmented alluvial fans in western Fresno County, California*. USGS Prof. Rep., P0352E: 89-128.

Benda L.E. & Cundy T.W. (1990) - *Predicting deposition of debris flows in mountain channels*. Canadian Geotechnical Journal, **27**: 409-417.

Bathurst J. C., Burton A. & Ward T. J. (1997) - *Debris flow run-out and landslide sediment delivery model tests*. Journal of Hydraulic Engineering, ASCE, **123**(5): 410-419.

Berti M. & A. Simoni. (2007) - *Prediction of debris flow inundation areas using empirical mobility relationships*. Geomorphology, **90**(**1**-**2**): 144-161.

Cannon S.H. (1989) - *An approach for estimating debris flow runout distance*. In: Proceedings Conference XX, International Erosion Control Association, Vancouver, British Columbia:457-468.

C.L Shieh & Y.F Tsai.(1998)- T*he 3-D deposition evolution of debris-flow fans.* Journal of the Chinese Institute of Civil and Hydraulic Engineering, **10**(**4**): 719-730.

Christine L.M. & Robert E.G. (2003) - *Spatial and temporal patterns of debris-flow deposition in the Oregon Coast Range, USA*. Geomorphology, *1362*: 1-15.

Fannin R.J. & Wise M.P. (2001) - *An empirical-statistical model for debris flow travel distance*. Canadian Geotechnical Journal, **38**: 982-994.

Ikeya H. (1981) - *A method of designation for area in danger of debris flow.* Erosion and Sediment Transport in Pacific Rim Steeplands, Proc., Int. Assoc. Hydro. Sci. Symp., IAHS Publ:576-588.

Iverson R.M., Schilling S.P. & Vallance, J.W. (1998) - *Objective delineation of lahar-inundation zones*. Geological Society of America Bulletin, **110**(**8**): 972-984.

Liu X.L & Mo D.W. (2002)- *Debris flow risk and site-specific debris flow risk assessment.* Journal of Engineering Geology, **10**(**03**): 266-273.

Lancaster S.T. (2003) - *Effects of wood on debris flow runout in small mountain watersheds*. Water Resources Research, **39**(**6**) :1168.

Perla R., Cheng T.T. & McClung D.M. (1980) - *A two parameter model of snow avalanche motion*. Journal of Glaciology, **26** (**94**): 197-208.

Pierson T.C. (1995) - *Flow characteristics of large eruption-triggered debris flows at snow-clad volcanoes: Constraints for debris-flow model*. Journal of Volcanology and Geothermal Research, **66**: 283-294.

Tang C., Liu X.L.n & Zhu J. (1993)- *The evaluation and application of risk degree for debris flow inundation on alluvial fans.* Journal of Natrual Disasters, **2**(**4**): 79-84.

Toyos G., Oramas Dorta D., et alii (2007) - *GIS-assisted modeling for debris flow hazard assessment based on the events of May 1998 in the area of Sarno, Southern Italy. Part 1: Maximum run-out.* Earth Surface Processes and Landforms, **32**(**10**): 1491-1502.

Whipple X.K. (1992) - *Predicting Debris-flow Runout and Deposition on Fans: the Importance of the Flow Hydrograph. Erosion, Debris Flows and Environment in Mountain Regions* (Proceedings of the Chengdu Symposium, July 1992) ,IAHS Publ., **209**: 337-345.

Zimmermann M. (1991) - *Formation of debris flow Cones: Results form Model Tests.* JAPAN-U.S.Workshop on Snow Avalanche,Landslide,Debris Flow Prediction and Control,Proc.JUWSLDPC:463-470

